

1 **Deriving probabilistic soil distribution coefficients ( $K_d$ ). Part 2: Reducing**  
2 **caesium  $K_d$  uncertainty by accounting for experimental approach and soil**  
3 **properties**

4 Oriol Ramírez-Guinart<sup>a</sup>, Daniel Kaplan<sup>b</sup>, Anna Rigol<sup>\*,a</sup>, and Miquel Vidal<sup>a</sup>

5 <sup>a</sup> *Chemical Engineering and Analytical Chemistry Department, Faculty of Chemistry,*  
6 *University of Barcelona, Martí i Franqués 1-11, 08028, Barcelona, Spain.*

7 <sup>b</sup> *Savannah River National Laboratory, Aiken, South Carolina, USA*

8

9 \*Corresponding author: Telephone: (+34) 93 403 9274; Fax: (+34) 93 402 1233

10 Email address: annarigol@ub.edu (A. Rigol)

11

12

13 **Acknowledgements**

14 This work was carried out in the frame of the IAEA MODARIA and MODARIA II  
15 programmes. It was supported by the Ministerio de Ciencia e Innovación de España  
16 (CTM2014-55191 and CTM2017-87107-R), the Generalitat de Catalunya (AGAUR  
17 2014SGR1277), and the Department of Energy's Office of Sciences, Subsurface  
18 Biogeochemistry Research Program (DE-AD09-96SR18500), and the Savannah River  
19 National Laboratory's LDRD program (LDRD-2017-00005). Oriol Ramírez-Guinart would  
20 like to thank the support of an APIF pre-doctoral fellowship from the University of  
21 Barcelona. Authors would also like to thank Dr. Brenda Howard for their fruitful discussions  
22 and Oriol Toll for his contribution in data treatment.

23

# 1 Deriving probabilistic soil distribution coefficients ( $K_d$ ). Part 2: Reducing 2 caesium $K_d$ uncertainty by accounting for experimental approach and soil 3 properties

## 4 5 **Abstract**

6 The solid-liquid distribution coefficient ( $K_d$ ) is a key input parameter in radioecological  
7 models. However, its large variability hampers its usefulness in modelling transport processes  
8 as well as its accuracy in representing soil-radionuclide interactions. For the specific case of  
9 radiocaesium, the analyses of a Cs  $K_d$  soil dataset (769 entries) showed that values varied over  
10 a five order of magnitude range, and the resulting Cs  $K_d$  best estimate (calculated as a  
11 geometric mean =  $2.5 \times 10^3 \text{ L kg}^{-1}$ ) lacked reliability and representativity. Grouping data and  
12 creation of partial datasets based on the experimental approach (short-term ( $< \sim 1 \text{ yr}$ ) vs. long-  
13 term experiments ( $> \sim 1 \text{ yr}$ )) and soil factors affecting Cs interaction (i.e., the ratio of the  
14 radiocaesium interception potential (RIP) to the potassium content in soil solution ( $K_{ss}$ );  
15 organic matter content (OM) and soil texture) succeeded in reducing variability a few orders  
16 of magnitude, with Cs  $K_d$  best estimates also differing by one-two orders of magnitude  
17 depending on the type of soil and experimental approach. The statistical comparison of the Cs  
18  $K_d$  best estimates and related cumulative distribution functions of the partial datasets revealed  
19 a relevant effect of the sorption dynamics on Cs  $K_d$  values (with long-term values  
20 systematically higher than short-term ones), and that the RIP/ $K_{ss}$  ratio was an excellent  
21 predictor of Cs  $K_d$  for short-term scenarios, whereas the RIP parameter could be predicted on  
22 the basis of texture information. The OM threshold to distinguish between Mineral and Organic soils subclasses, regarding Cs interaction was  
23 determined to be 50% and 90% OM for short- and long-term scenarios, respectively. It was  
24 then recommended to select the Cs  $K_d$  input data depending on the soils and scenarios to be  
25 assessed (e.g., short- vs. long-term; OM %) to improve the reliability and decrease the  
26 uncertainty of the radioecological models.  
27

## 28 29 **Keywords**

30 Distribution coefficient; soil; cumulative distribution function; radiocaesium; radiocaesium  
31 interception potential; probabilistic modeling

32

## 33 1. Introduction

34 Radiocaesium (Cs) interaction with soils and other materials like clays has been thoroughly  
35 studied in the last couple decades, which has led to a strong understanding of the sorption  
36 mechanisms governing Cs sorption in soils and to the identification of related soil  
37 physicochemical properties (Comans et al., 1989; Cremers et al., 1990; Vidal et al., 1995;  
38 Rigol et al., 1998; Okumura et al., 2018). Cs speciation in solution is very simple. In the  
39 natural environment, the predominant Cs species in solution are hydrolysed cations, and thus  
40 Cs-soil interaction is based on cation exchange reactions involving two main types of sorption  
41 sites with contrasting affinity for Cs and selectivity for monovalent and divalent cations. In  
42 those soils with high organic matter content and absence of 2:1 phyllosilicates, Cs sorption is  
43 mainly caused by the interaction with regular exchange sites (RES) (Rigol et al., 1998; Rigol  
44 et al., 2002). RES are present in organic matter and clay minerals as a result of deprotonation  
45 of certain functional groups and isomorphic substitutions, respectively; and they can be  
46 roughly estimated with soil cation exchange capacity (CEC). Since RES have low affinity and  
47 low selectivity coefficients for monovalent cations (*e.g.*, Cs/K or Cs/NH<sub>4</sub><sup>+</sup>), Cs sorption in  
48 RES is considered as a weak and non-specific interaction (Vidal et al., 1995) that can be  
49 highly inhibited by the presence in solution of other monovalent cations and, specially,  
50 divalent cations presenting a higher electrostatic affinity, due to sorption competition  
51 processes (Comans et al., 1989; Cremers et al., 1990). When only trace levels of 2:1  
52 phyllosilicates are present in soils, Cs sorption becomes controlled by its interaction with  
53 sorption sites located in the interlayer space of these minerals, which include illite,  
54 vermiculite or smectite and, particularly, in the frayed edge sites (FES). FES have an  
55 extremely high-affinity for monovalent cations (described in below) (Cremers et al., 1988;  
56 Okumura et al., 2018). In this context, a prediction of the Cs K<sub>d</sub> may be attempted on the basis  
57 of the following equation (Gil-Garcia et al., 2011):

$$59 K_d = K_d^{FES} + K_d^{RES} = \frac{RIP_K}{K_{ss} + K_C^{FES}(NH_4/K) \cdot NH_{4,ss} + K_C^{FES}(Na/K) \cdot Na_{ss}} + \frac{K_{exch} + NH_{4,exch} + Na_{exch}}{K_{ss} + NH_{4,ss} + Na_{ss}} \quad [1]$$

60  
61 in which RIP<sub>K</sub> is the Radiocaesium Interception Potential (RIP) obtained by measuring the  
62 amount of caesium sorbed in a medium containing 100 mmol L<sup>-1</sup> of Ca and 0.5 mmol L<sup>-1</sup> of  
63 K (Wauters et al., 1996), K<sub>ss</sub>, NH<sub>4,ss</sub> and Na<sub>ss</sub> refer to K, NH<sub>4</sub><sup>+</sup> and Na concentrations in soil  
64 solution, K<sub>exch</sub>, NH<sub>4,exch</sub> and Na<sub>exch</sub> stand for K, NH<sub>4</sub><sup>+</sup> and Na concentrations in the  
65 exchangeable complex, and K<sub>C</sub><sup>FES</sup> is the monovalent trace selectivity coefficients at FES.

66  $K_C^{FES}$  (Na/K) takes a value around 0.02, whereas  $K_C^{FES}$  (NH<sub>4</sub>/K) roughly varies within a 4-8  
67 range. This equation can be simplified by only considering the  $RIP_K$ , that accounts for the  
68 soil capacity to specifically sorb Cs (Sweeck et al., 1990; Wauters et al., 1996), and the K  
69 concentration in the soil solution, as key soil properties governing Cs  $K_d$  values, specifically  
70 when sorption at RES can be disregarded, as illustrated in the Equation 2 (Gil-Garcia et al.,  
71 2011):

$$72$$
$$73 K_d^{FES} = RIP_K / K_{ss} \quad [2]$$
$$74$$

75 The specific Cs sorption,  $K_d^{FES}$ , is crucial for the understanding the long-term Cs-soil  
76 interaction, which is the result of complex Cs-clays multiple reactions, especially with illite,  
77 montmorillonite and mordenite clays (de Koning and Comans, 2004; Ohnuki and Kozai,  
78 2013; Durrant et al., 2018; Okumura et al., 2018). Sorbed Cs species undergo a progressive  
79 dehydration reaction with time that causes the so-called clay interlayer spacing collapse and  
80 implies that the dehydrated sorbed Cs may become trapped in the clay bulk (Wampler et al.  
81 2012; Fuller et al., 2015). Because of this, Cs sorption to FES is a slow dynamic process,  
82 resulting in the fraction of sorbed Cs that virtually is irreversibly sorbed and no longer  
83 participates in the partition between the solid and liquid phases to increase with time. This  
84 process is known as sorption aging and enhances the fraction of irreversibly bound Cs  
85 (Absalom et al., 1995; Roig et al., 2007; Wang and Staunton, 2010; Wampler et al. 2012  
86 Söderlund et al., 2016). Therefore, important considerations affecting the risk posed by Cs  
87 contaminated soils is whether there has been a short or long Cs contact time with the soil and  
88 whether 2:1 clays are present.

89

90 The  $K_d$  parameter is used in many radioecological risk assessment models for multiple  
91 purposes, including estimating radionuclide transport, plant-soil partitioning, and desorption  
92 from a source term (Krupka et al. 1999; Almahayni et al, 2019).  $K_d$  values are used to  
93 determine radionuclide partitioning between the dissolved and solid phases and when  
94 combined with the bulk density and porosity of the soil it can be used to calculate the  
95 retardation factor (Krupka et al. 1999), which in turn can be used to estimate the mobile  
96 radionuclide fraction (Krupka et al. 1999). In an identical calculation but with a different  
97 intent, the  $K_d$  can be used to estimate the release of radionuclides from a contaminated source.  
98  $K_d$  values may also be used to estimate the plant to soil concentration ratio based on the  
99 assumption that plants take up primarily radionuclides from the porewater solution phase, as

100 estimated by the denominator of the  $K_d$ . Users can estimate external doses to organisms by  
101 inputting either soil or water radionuclide activity concentrations, and then the model  
102 estimates the associated soil or water radionuclide activity concentration through the use of  $K_d$   
103 values (Beaugelin-Seiller et al., 2002; Brown et al., 2016).  $K_d$  values can be used to estimate  
104 leaching of a radionuclide from a surface soil to an underlying zone (e.g., vadose zone or  
105 aquifer) by accounting for both plant uptake (plant:soil partitioning) and sorption during  
106 transport (retardation factor). Finally, in semi-mechanistic models focusing in Cs, specific  
107 parameters such as RIP can also be used to internally predict Cs  $K_d$  values (Equation 2)  
108 (Absalom et al, 2001; Tarsitano et al., 2011). In each of these uses of the  $K_d$  parameter, data  
109 can be entered as a single value or as a probability density function (Simon-Cornu et al.,  
110 2015).

111  
112 This work is the second in an initial series of three publications (Ramírez-Guinart et al.,  
113 2020a; Ramírez-Guinart et al., 2020b) aiming at deriving sorption data suitable for risk  
114 assessment from soil  $K_d$  datasets, as well as to develop a strategy to reduce and describe  $K_d$   
115 variability based on probabilistic models, including the construction of distribution functions  
116 to statistically describe the  $K_d$  values of a target radionuclide (RN), in this case radiocaesium.  
117 As explained in part 1 (Ramírez-Guinart et al., 2020a), the International Atomic Energy  
118 Agency (IAEA)  $K_d$  dataset described in Technical Reports Series Number 472 (TRS-472;  
119 IAEA, 2010) was the starting point of the work. Under the auspices of the IAEA-MODARIA  
120 (Modelling and Data for Radiological Impact Assessment) project, the TRS-472 dataset was  
121 updated and critically reviewed following agreed acceptance criteria by the MODARIA  
122 Working Group 4, including: 1) rejecting any  $K_d$  value not directly quantified as the ratio  
123 between concentrations of the target element measured in a liquid and a solid phase (i.e.,  
124 reject data from parametric equations, mass-transport experiments, or  $K_d$  reference values  
125 were excluded); 2) rejecting  $K_d$  values created by pooling values originating from varying  
126 non-relevant operational or soil variables; 3) excluding values obtained from experiments not  
127 representative for environmental conditions (such as extremely low or high pH); 4) accepting  
128 data from stable isotopes obtained at the lowest concentration range; and 5) rejecting data  
129 from pure (soil) mineral phases, such as clay minerals or metal (hydro)oxides. The resulting  
130 critically reviewed dataset contains >7000 soil  $K_d$  entries for 83 elements (Ramírez-Guinart et  
131 al., 2020a), of which 769 entries describe soil Cs  $K_d$  values.

132 Previous work has derived Cs  $K_d$  best estimate values from large datasets, as well from partial  
133 datasets created based on the RIP parameter and texture and organic matter content (Gil-  
134 Garcia et al., 2009). The objectives of this study are to evaluate and quantify new potential  
135 sources of variability of Cs  $K_d$  values. More specifically, the objectives of this study were: 1)  
136 to evaluate if Cs contact time with soil (i.e., short-term vs. long-term;  $< \sim 1$  yr and  $> \sim 1$  yr,  
137 respectively) affects Cs  $K_d$  values and therefore be a source for Cs  $K_d$  variability; 2) to  
138 evaluate several groupings aligned with various soil properties, including RIP/ $K_{ss}$ , and soil  
139 OM+Texture; 3) because RIP is not commonly measured, evaluate whether it can be  
140 estimated by common soil texture properties; and 4) to determine the organic matter (OM)  
141 content threshold to optimally distinguish between mineral and organic soils to permit  
142 reducing Cs  $K_d$  uncertainty. The intent of this study was not only to identify significant  
143 differences between these various soil categories, but also to improve present approaches to  
144 selecting Cs  $K_d$  values to minimize uncertainty, thereby improving input data of  
145 radioecological models.

146

## 147 **2. Data collection and treatment**

148

### 149 *2.1. Current status of the Cs $K_d$ compilation*

150 The updated MODARIA Cs dataset contains 769 entries with related soil characteristics and  
151 details regarding the experimental approach (Ramírez-Guinart et al., 2020a). With respect to  
152 the TRS-472 compilation, a significant set of data gathered from desorption experiments of  
153 indigenous Cs has been integrated because of the changes introduced in data acceptance  
154 criteria (POSIVA, 2014; SKB, 2014). The soil Cs  $K_d$  overall dataset contained values ranging  
155 within up to five orders of magnitude (Min-Max range of  $4 \times 10^0$  -  $4.5 \times 10^5$  L kg<sup>-1</sup>). The large  
156 Cs  $K_d$  variability of the dataset denotes the presence of data from soils with contrasting key  
157 properties (e.g., RIP, OM, clay content, K in soil solution, etc.) and from different  
158 experimental approaches.

159 Besides fields within the dataset related to the sources of information, radioisotopes, soil  
160 characteristics and ancillary information (such as pH, organic matter content, cationic  
161 exchange capacity (CEC), clay and sand contents referred to mineral matter; exchangeable K  
162 and NH<sub>4</sub>; concentration of K and NH<sub>4</sub> in soil solution; and RIP), additional fields were  
163 included related to the experimental approach (either short or long-term experiments).

164

165 *2.2. Soil factors and developed criteria to group Cs K<sub>d</sub> data*

166 Cs K<sub>d</sub> values have to be grouped according to soil factors specific to the Cs sorption  
167 mechanisms. As discussed above, the Cs K<sub>d</sub><sup>FES</sup>, which is equal to the RIP/K<sub>ss</sub> (Eq. 2), was  
168 used as a criterion for reducing Cs K<sub>d</sub> variability (Gil-García et al., 2009). Four RIP/K<sub>ss</sub>  
169 ranges were created:  $RIP/K_{ss} < 10^2$  ;  $10^2 \leq RIP/K_{ss} < 10^3$ ;  $10^3 \leq RIP/K_{ss} < 10^4$ ; and  
170  $RIP/K_{ss} > 10^4$ , as previously agreed in past analyses (IAEA, 2009).

171  
172 Ideally the soil factor used to categorize soils for predicting Cs K<sub>d</sub> values would be based  
173 directly on the concentration of the 2:1 clay minerals that provide FES, rather than RIP.  
174 However, such measurements are costly (involving multiple X-ray diffraction analyses of a  
175 single soil sample) and are typically not conducted in routine soil analyses. Consequently,  
176 few mineralogy characterisation data are available for soils, thus making any mineralogy-  
177 based grouping criteria of limited practical use. Thus, a K<sub>d</sub> grouping criterion based on the  
178 soil texture and OM content, the so-called OM+Texture criterion previously defined and  
179 agreed upon (IAEA, 2010), was also applied to group Cs K<sub>d</sub> data. In short, a Cs K<sub>d</sub> value was  
180 included in the organic group if the soil had an OM content  $\geq 20\%$ , whereas it was included in  
181 the Mineral group if OM was lower than 20%. Secondly, the K<sub>d</sub> data contained in the Mineral  
182 group were split in three textural groups (Sand, Loam, and Clay) when textural data were  
183 available. Based on percentage of the mineral fraction, the Sand group was defined by a sand  
184 fraction  $\geq 65\%$ , and a clay fraction  $< 18\%$ ; Clay group: clay fraction  $> 35\%$ ; and Loam group,  
185 rest of cases. The suitability of the OM+Texture K<sub>d</sub> grouping criterion to propose soil-type  
186 Cs K<sub>d</sub> data lies on the fact that even though the OM+Texture criterion is not based on the  
187 fundamental description of the underlying sorption processes of Cs in soils, it partially  
188 captures some of the soil properties that can play a key role in the Cs-soil interaction.

189  
190 The OM threshold traditionally used to discern between an organic and a mineral soil may not  
191 be the most appropriate for Cs K<sub>d</sub>. A 20% OM threshold to distinguish between soils with a  
192 high Cs sorption capacity due to the presence of the mineral fraction and those with a low  
193 sorption capacity due to the absence of FES could not be appropriate, as a minor content of  
194 mineral fraction can govern Cs sorption even in organic soils such as histosols (Vidal et al.,  
195 1995; Rigol et al., 1998). Therefore, the effect of varying the OM concentration threshold was  
196 also analysed to redefine the OM+Texture criterion.

197

198 *2.3. Analysis of the influence of the experimental approach on Cs  $K_d$  data variability*

199 As with other papers in this series, the influence of the experimental approach was  
200 simultaneously evaluated along with relevant soil factors for reducing Cs  $K_d$  variability. From  
201 the three experimental approach categories (short-term sorption (ST-S), short-term desorption  
202 (ST-D), and long-term desorption (LT-D)) (Ramirez-Guinart et al., 2020a), the greatest  
203 number of  $K_d$  entries were in the “short-term sorption” category (that is, Cs  $K_d$  derived from  
204 applying a sorption batch test based on putting in contact for short times a non-contaminated  
205 soil with a solution spiked with radiocaesium or with low concentrations of stable Cs), and  
206 “long-term desorption” (that is,  $K_d$  of anthropogenic Cs derived from applying an extraction  
207 test to long-term contaminated solid materials with radiocaesium, or  $K_d$  derived from  
208 indigenous Cs from performing an extraction test when the total content of the indigenous Cs  
209 at the solid matrix is quantified). There were no entries that could be considered as “short-  
210 term desorption data” (Cs  $K_d$  derived from anthropogenic radiocaesium from applying an  
211 extraction batch test to soils recently contaminated with radiocaesium). Therefore, according  
212 to the entries available for the experimental approach categories, only the differences between  
213 the overall short-term versus long-term datasets were finally examined.

214

215 The data treatment was based on group mean centering (GMC) to minimize the effect of soil  
216 factors on the interaction terms and to examine better the individual role of the experimental  
217 approaches on Cs  $K_d$  variability (Bell et al., 2018). Regarding soil factors and based on the  
218 previous experience of similar grouping exercises (Gil et al., 2009), these analyses could be  
219 carried out by either considering the RIP/ $K_{ss}$  or the OM+Texture criteria. For the GMC  
220 treatment, the use of the RIP/ $K_{ss}$  factor was dismissed as the RIP concept accounts for short-  
221 term and reversible sorption scenario. Therefore, the GMC was only addressed to minimize  
222 the effect of OM and texture on elucidating the role of the experimental approach factor.  
223 Firstly, the overall Cs dataset was log-transformed, the log Cs  $K_d$  data was then grouped  
224 according to the OM+Texture criterion. The arithmetic mean (AM) of the log Cs  $K_d$  values of  
225 each soil-type group was calculated and each log Cs  $K_d$  value within a given group was  
226 corrected by subtracting the AM log Cs  $K_d$  value of the respective soil-type group.  
227 Subsequently, the GMC-corrected log Cs  $K_d$  datasets were divided according to the type of  
228 the experimental approach and statistical tests (Fisher’s least significant differences (FLSD)  
229 test for multiple means; 95% confidence level; StatGraphics 18) were performed to check  
230 whether the Cs  $K_d$  means for each experimental approach significantly differed.



231

#### 232 *2.4. Construction of cumulative distribution functions to describe Cs K<sub>d</sub> variability*

233 Cumulative Distribution Functions (CDF) of Cs K<sub>d</sub> data were constructed to describe the  
234 population and variability of each groupings' datasets. Since the K<sub>d</sub> parameter is a ratio of  
235 concentrations, K<sub>d</sub> data are expected to follow a lognormal distribution (Sheppard et al.,  
236 2011). Thus, lognormal was the first function distribution of the Cs K<sub>d</sub> data tested. For the  
237 construction of CDFs, Cs K<sub>d</sub> data were log-transformed and the presence of possible outlier  
238 values in the datasets was examined by performing an exploratory analysis based on box-and-  
239 whisker plots. The log Cs K<sub>d</sub> data within every dataset were sorted by increasing value and an  
240 empirical frequency ( $f_{\text{exp},i}$ ) equal to  $1/N$  (where  $N$  is the total number of Cs K<sub>d</sub> entries in the  
241 respective dataset) was assigned to each entry. Experimental group cumulative frequency  
242 distributions were constructed by assigning to each sorted log Cs K<sub>d</sub> value their corresponding  
243 cumulative frequency ( $F_{\text{exp},i}$ ), *i.e.*, the sum of the preceding frequencies  
244 ( $F(K_{d,j}) = \sum_{i=0}^j f(K_{d,i})$ ). The Kolmogorov-Smirnov test was then applied to ascertain whether  
245 the underlying frequency distribution in each Cs K<sub>d</sub> dataset was significantly different from  
246 the lognormal distribution. As expected, it was confirmed that overall and partial Cs K<sub>d</sub>  
247 datasets followed a lognormal distribution. Consequently, the experimental cumulative  
248 frequency distributions constructed with the log Cs K<sub>d</sub> data were fitted to the theoretical  
249 normal CDF equation, and the related geometric mean (GM) and percentile ranges were  
250 derived. Further details can be found elsewhere (Ramírez-Guinart et al., 2020a).

251

252 To derive properly a reliable CDF from a given K<sub>d</sub> dataset it is necessary that it contains a  
253 minimum number of entries ( $N \approx 10$ ). However, there were a few partial datasets containing  
254 less than 10 entries for which CDFs were evaluated. Those partial datasets that provided a  
255 good fit to the lognormal distribution were reported and for the rest of the cases only GM  
256 values were calculated.

257

### 258 **3. Analyses of Cs K<sub>d</sub> distributions**

259

#### 260 *3.1. Influence of the experimental approach on Cs K<sub>d</sub> data*

261 The overall Cs K<sub>d</sub> dataset contained K<sub>d</sub> data gathered by applying sorption experiments in a  
262 short-term scenario (ST-S), and desorption experiments in a long-term scenario (LT-D).

263 When the statistical analysis was performed after applying the GMC to the partial datasets

264 created from the application of the OM+Texture criterion, significant differences were  
265 observed between ST-S and LT-D (data not shown). Thus, short-term and long-term Cs  $K_d$   
266 data must be distinguished before testing any further grouping criteria, which agrees with the  
267 fact that long-term incorporated Cs may undergo an aging process leading to an increase in  
268 the Cs sorption irreversibility.

269

270 Figure 1 shows the Cs  $K_d$  descriptors of the distributions of the short-term and long-term  
271 partial datasets from the overall dataset, as well as the related CDFs. The Cs  $K_d$  data and  
272 CDFs for the long-term incorporated Cs (GM and 5<sup>th</sup> – 95<sup>th</sup> percentile range values) were an  
273 order of magnitude or more greater than those of short-term. An implication of this finding is  
274 that the use of long-term Cs  $K_d$  data should be avoided to predict soil Cs sorption behaviour in  
275 recently contamination systems, and *vice versa*, values from short-term measurements of Cs  
276  $K_d$  should be avoided to predict long-term Cs sorption behaviour.

277

### 278 3.2. Cs $K_d$ best estimates and CDFs based on the RIP/ $K_{ss}$ criterion

279 Of the 769 entries in the Cs  $K_d$  dataset, 328 contained sufficient ancillary information for  
280 calculating the RIP/ $K_{ss}$ . The log-log correlation between experimental Cs  $K_d$  and the  
281 respective RIP/ $K_{ss}$  values could explain 64% of the total Cs  $K_d$  variance, representing a  
282 profound result considering the large variability of the dataset (see equation 3 and Figure S1  
283 in the Supplementary Material):

284

$$285 \log K_d = 0.76 (\pm 0.18) + 0.73 (\pm 0.06) \times \log(\text{RIP}/K_{ss}) \quad (N = 328; r = 0.80; p = 2.6 \times 10^{-74}) \quad [3]$$

286

287 In this context, the construction of the CDFs helps to describe the variability associated with  
288 the use of the RIP/ $K_{ss}$  ratio, to propose Cs  $K_d$  best estimates derived from the use of the  
289 RIP/ $K_{ss}$  criterion, and to quantify their uncertainty.

290

291 Figure 2 depicts the graphical representation of the CDFs constructed from each partial  
292 dataset created by applying the RIP/ $K_{ss}$  criterion as well as the main quantitative outcomes  
293 from the CDF construction. The Cs  $K_d$  GMs and related 5<sup>th</sup>-95<sup>th</sup> percentile ranges increased  
294 when increasing each RIP/ $K_{ss}$  group. Whereas the examination of the Cs  $K_d$  GM is of a lesser  
295 importance in this case (as an end-user with available RIP and  $K_{ss}$  data can straightforwardly  
296 calculate an approximate, related Cs  $K_d$  value), the 5<sup>th</sup>-95<sup>th</sup> percentiles permit to quantify and  
297 describe the Cs  $K_d$  variability within each dataset. The variability in the partial datasets was

298 only of one to two orders of magnitude. Besides, the constructed CDFs curves did not overlap  
299 among them. Therefore, the calculation of the  $RIP/K_{ss}$  ratios permits a rapid estimation of the  
300  $C_s K_d$ , with an associated uncertainty calculated from the corresponding CDF.

301

302 A major limitation of this approach lies on the fact that it is necessary to have the soil RIP  
303 value, a parameter that albeit being more and more frequently determined it is not yet  
304 characterised on routine analyses. Therefore, end-users may find useful an equation enabling  
305 the prediction of soil RIP values from soil properties often available or, at least, much easier  
306 to determine than the RIP parameter. Previous studies demonstrated that RIP values can be  
307 roughly predicted from soil clay and silt contents (Waegeneers et al. 1999; Gil-García et al.,  
308 2011). Here, a multiple linear regression is created from data from the current compilation as  
309 well as from data from other works in which RIP was measured along with other soil  
310 properties (Vandebroek et al., 2012; Uematsu et al., 2015). The correlation captured around  
311 70% of total RIP variability and reliably correlated RIP values of soils with their clay and silt  
312 contents:

313

$$314 \log RIP = 1.24 (0.09) + 0.76 (0.06) \times \log Clay + 0.68 (0.06) \times \log Silt \quad (N = 225; r = 0.82; p =$$
$$315 1.4 \times 10^{-54}) \quad [4]$$

316

317 This model could be improved if the 2:1 phyllosilicates content would be quantified (Nakao et  
318 al., 2015; Uematsu et al., 2015), although this information is expensive and not available in  
319 routine analyses. Thus, the development of an equation to predict RIP values not only from  
320 clay content but from clay mineralogy remains a future challenge.

321

322 A secondary limitation of this approach is that the K concentration in the soil solution is not  
323 routinely analysed by researchers. However, there have been a few attempts to estimate this  
324 parameter from other soil properties, such as from exchangeable K and  $K K_d$  estimates reported  
325 for mineral and organic soils; from the total K content, the CEC in clay minerals and from the  
326 percentage of the exchange sites on soil clay minerals occupied by K. In the case of organic  
327 soils, the gravimetric humus content of the soil is also required as well as to distinguish between  
328 CEC of humus and clay sites (Absalom et al., 2001; Gil-García et al., 2009).

329 *3.3. Cs  $K_d$  best estimates and CDFs based on the OM+Texture criterion*

330 *3.3.1. Cs  $K_d$  best estimates and CDFs based on the initial OM+Texture criterion*

331 The Cs  $K_d$  dataset, refined to include those entries with the information required for the  
332 OM+Texture criterion, contained 573 entries, an additional 100 entries compared to the TRS-  
333 472 dataset (IAEA, 2010). Table 1 summarises the Cs  $K_d$  data obtained from the CDFs  
334 constructed by applying the OM+Texture criterion, distinguishing between short- and long-  
335 term partial datasets, as well as by mineral and organic soils, and when statistically  
336 significant, textural classes within the mineral soils.

337 With the short-term data, the GMs derived from the CDFs created with the short-term data  
338 evidenced that Cs  $K_d$  values for the Mineral dataset were statistically greater than that of the  
339 Organic dataset. Within the Mineral dataset, the  $K_d$  GMs increased along with the soil clay  
340 content ( $GM_{\text{sand}} < GM_{\text{loam}} < GM_{\text{clay}}$ ). However, and although kept separately in the table, Clay  
341 and Loam datasets were not significantly different. This pattern is generally consistent with  
342 reported Cs sorption mechanisms, Cs partitioning between FES and RES sites and the  
343 relatively weak sorption of Cs to natural OM sites (Rigol et al., 2002). For the long-term data,  
344 the GM derived for the Mineral group was also one order of magnitude higher than that of the  
345 Organic group, although no statistical differences were observed among the textural groups  
346 among them and with respect to the Mineral dataset.

347

348 The GM values (Table 1) derived from the Mineral soil group created from the short-term  
349 dataset was statistically lower than that of the long-term dataset (more than one order of  
350 magnitude) and the 5<sup>th</sup>-95<sup>th</sup> intervals of the long-term Mineral dataset were shifted to higher  
351 Cs  $K_d$  values, which corroborates the influence of the sorption dynamics on the Cs  $K_d$  values  
352 as observed in the Section 3.1. Moreover, the same pattern was also observed for the Organic  
353 datasets, as the GM values of the Organic dataset in the long-term scenario was one order of  
354 magnitude higher than that of the short-term. This may indicate that the 20% OM content  
355 threshold to distinguish between mineral and organic soils regarding Cs interaction is too low  
356 for this radionuclide. This observation may be attributed to FES out competing the RES that  
357 account for Cs sorption to OM (Rigol et al., 1998; Roig et al, 2007).

358

359 The comparison of the 5<sup>th</sup>-95<sup>th</sup> percentile ranges of Cs  $K_d$  values obtained from the  
360 OM+Texture partial datasets with that of the overall Cs  $K_d$  dataset indicates that the  
361 application of the OM+Texture criterion to short-term data allowed us to create Cs  $K_d$  mineral  
362 textural groups with a much lower variability (lower GSD and more narrow percentile ranges)

363 than that of the overall data set (down to one-to-two orders of magnitude in a few cases)  
364 (Table 1). Conversely, organic soils datasets contained Cs  $K_d$  values still varying within  
365 ranges similar to those of overall short- and long-term datasets. Thus, these results suggest  
366 that the initial OM+Texture criterion could be improved by better establishing the OM%  
367 threshold for Cs to distinguish between mineral and organic soils.

368

### 369 *3.3.2. Cs $K_d$ best estimates and CDFs based on the redefined OM+Texture criterion*

370 The effect of changing the OM thresholds to better distinguish between mineral from organic  
371 soils were tested for short- and long-term partial Cs  $K_d$  datasets. Criteria to select the new OM  
372 thresholds were based on 1) to analyse significant changes in the derived Cs  $K_d$  GMs; 2) to  
373 obtain organic and mineral soil distributions with enough entries and minimum variability;  
374 and 3) to obtain similar Cs  $K_d$  best estimates for short- and long-term organic soil datasets.

375

376 A few entries were excluded if the OM content was not reported. As summarized in Table S1  
377 in the Supplementary Material, the GMs of the Mineral datasets were statistically the same  
378 regardless the OM threshold, whereas the GMs from the Organic datasets progressively  
379 decreased by increasing the OM threshold up to 50%, and remained statistically constant for  
380 the 60% OM threshold. Besides this, the variability of the Mineral datasets was roughly the  
381 same for all the OM thresholds tested, whereas variability decreased significantly for the  
382 Organic datasets when increasing the OM threshold up to 50%, with no further improvement  
383 for the 60% threshold. Therefore, a 50% OM threshold is suggested for short-term datasets.

384

385 Regarding long-term data, data limitation required that we evaluate greater threshold values,  
386 up to 90%. The GM Cs  $K_d$  and related variability of the Mineral datasets remained constant  
387 regardless the OM threshold, whereas for the Organic datasets GMs and related variability  
388 were gradually decreased as the OM threshold value was increased. The decrease was  
389 statistically significant when the 90% OM threshold was applied. From these results, it is  
390 suggested a 90% OM content as a threshold to distinguish between organic and mineral soils  
391 for long-term data.

392

393 The third criterion for establishing the new thresholds was only partially achieved. Whereas  
394 the GM of the organic short-term and long-term datasets approached with the new thresholds  
395 (from one-order of magnitude difference to a lower 4 fold), the datasets were still statistically  
396 different at 95% confidence level, although with a  $p$  value of 0.043. Therefore, the two

397 datasets could be considered as comparable. However, greater organic datasets according to  
398 the redefined thresholds with more entries (especially for the long-term scenario) are needed  
399 to be able to statistically fulfil this criterion. If an overall short-term plus long-term organic  
400 dataset is built up with the redefined OM thresholds, with 45 entries, a best-estimate of  
401  $1.1 \times 10^2 \text{ L kg}^{-1}$  (GSD = 4.2) can be derived from the overall organic dataset.

402

403 Figure 3 summarises the Cs  $K_d$  data obtained from the CDFs constructed by applying the  
404 redefined OM+Texture criteria to the short-term and long-term partial datasets and the CDF  
405 graphical representations. The changes introduced concerning the OM thresholds resulted in  
406 partial datasets with much lower variability than when using the initial OM+Texture criterion.  
407 The derived Cs  $K_d$  GM values increased with increasing clay content leading to well-defined  
408 CDFs among textural groups, also for the long-term datasets. Besides, for a given textural soil  
409 group, the long-term Cs  $K_d$  data were systematically much higher (around one order of  
410 magnitude) than those corresponding to the short-term data.

411

412

#### 413 **4. Conclusions and recommendations**

414 From the analyses performed to the Cs  $K_d$  dataset, it was found that sorption dynamics effects  
415 (i.e., long-term vs. short-term scenarios) had a strong impact on the Cs  $K_d$  values and related  
416 variability. This fact should be taken into consideration when dealing with risk assessment  
417 exercises in which Cs  $K_d$  data are required. Besides, it was also evidenced that soil properties  
418 either directly related to the mechanisms governing Cs sorption in soils, like soil RIP and K  
419 concentration in soil solution, or indirectly related, such as the soil OM and to a lesser extent  
420 the soil texture, dramatically affected the Cs  $K_d$  values and their variability. These soil  
421 properties should be available for a proper estimation and selection of Cs  $K_d$ .

422

423 A single Cs  $K_d$  best estimate and/or CDF has little practical value for modelling because it is  
424 fraught with high variability and it is not assured that it is representative of the target scenario.  
425 Alternatively, it is highly recommended to end-users to select the Cs  $K_d$  best estimates and  
426 CDF that corresponds to their scenario of interest. First, it is crucial to identify if the  
427 assessment is made for a recent contamination episode such as right after a radioactive  
428 accidental release (short-term scenario,  $< \sim 1$  yr) or for a post-contamination episode that  
429 occurred a long time ago or for predictions extended to the future (e.g., in the context of  
430 safety and performance assessment of deep geological repositories or long-term impact

431 assessment of contamination episodes). If the radiological assessment exercise is done for a  
432 short-term scenario and the RIP and  $K_{ss}$  data are available for the studied soil, it is  
433 recommended to use a Cs  $K_d$  value based on the direct calculation of the RIP/ $K_{ss}$  ratio,  
434 associated with the uncertainty derived from the constructed CDF for the corresponding  
435 RIP/ $K_{ss}$  group, in which, if required, RIP can be predicted directly from the clay and silt  
436 contents of the soil.  $K_{ss}$  could also be derived from other soil properties, such as total K, and  
437 CEC of clay and humus fractions. Both from short- and long-term scenarios, if soil organic  
438 matter content of the target soil is known, it is suggested to use the CDF that also suits the soil  
439 type (Organic or Mineral), whereas if soil texture data is also available it is suggested to refine  
440 the CDF election also according to the textural group.

441

442

#### 443 **References**

444 Absalom, J. P., Young, S. D., Crout, N. M., 1995. Radio-caesium fixation dynamics:  
445 measurement in six Cumbrian soils. *Eur. J. Soil Sci.* 46, 461-469.

446 Absalom, J.P., Young, S.D., Crout, N.M.J., Sanchez, A., Wright, S.M., Smolders, E., Nisbet,  
447 A.F., Gillett, A.G., 2001. Predicting the transfer of radiocaesium from organic soils to  
448 plants using soil characteristics. *J. Environ. Radioact.* 52, 31–43.

449 Almahayni, T., Beresford, N.A., Crout, N.M.J., Sweeck, L. 2019. Fit-for-purpose modelling  
450 of radiocaesium soil-to-plant transfer for nuclear emergencies: a review. *J. Environ.*  
451 *Radioact.* 201, 58-66.

452 Beaugelin-Seiller, K., Boyer, P., Garnier-Laplace, J., Adam, C. 2002. Casteaur: a simple tool  
453 to assess the transfer of radionuclides in waterways, *Health. Phys.* 84, 539–542.

454 Bell, A.; Jones. K., Fairbrother, M. 2018. Understanding and misunderstanding group mean  
455 centering: a commentary on Kelley et al.'s dangerous practice. *Quality & Quantity* 52,  
456 2031–2036.

457 Brown, J.E., Alfons, B., Avila, R., Beresford, N.A., Copplestone, D., Hosseini, A. 2016. A  
458 new version of the ERICA tool to facilitate impact assessments of radioactivity on wild  
459 plants and animals, *J. Environ. Radioact.* 153, 141–148.

460 Comans, R. N., Middelburg, J. J., Zonderhuis, J., Woittiez, J. R., De Lange, G. J., Das, H. A.,  
461 Van der Weijden, C. H., 1989. Mobilization of radiocesium in pore water of lake  
462 sediments. *Nature* 339, 367-369.

463 Cremers, A., Elsen, A., De Preter, P., Maes, A., 1988. Quantitative analysis of radiocesium  
464 retention in soils. *Nature* 335, 247-249.

465 Cremers, A., Elsen, A., Valcke, E., Wauters, J., Sandalls, F. J., Gaudern, S. L., 1990. In:  
466 Desmet, G., Nassibeni, P., Belli, M. (Eds.) *Transfer of radionuclides in natural and semi-*  
467 *natural environments*, New York, USA: Elsevier Applied Science Publishers.

468 de Koning, A., Comans, R. 2004. Reversibility of radiocaesium sorption on illite. *Geochem.*  
469 *Cosmochim. Acta*, 68, 2815-2823.

470 Durrant, C.B., Begg, J.D., Kersting, A.B., Zavarin, M. 2018. Cesium sorption reversibility  
471 and kinetics on illite, montmorillonite, and kaolinite. 2018. *Sci. Total Environ.* 610–  
472 611, 511-520.

473 Fuller, A.J., Shaw, S., Ward, M.B., Haigh, S.J., Mosselmans, J.F.W., Peacock, C.L.,  
474 Stackhouse, S., Dent, A.J., Trivedi, D., Burke, I.T. 2015. Caesium incorporation and  
475 retention in illite interlayers. *Appl. Clay Sci.* 108, 128-134.

476 Gil-García, C., Rigol, A., Vidal, M., 2009. New best estimates for radionuclide solid–liquid  
477 distribution coefficient in soils. Part 1: radiostrontium and radiocaesium. *J. Environ.*  
478 *Radioact.* 100, 690–696.

479 Gil-García, C., Rigol, A., Vidal, M., 2011. Comparison of mechanistic and PLS-based  
480 regression models to predict radiocaesium distribution coefficients in soils. *J. Hazard. Mat.*  
481 197, 11– 18.

482 IAEA, 2009. TECDOC-1616 - Quantification of radionuclide transfer in terrestrial and  
483 freshwater environments for radiological assessments. International Atomic Energy  
484 Agency, Austria.

485 IAEA, 2010. TRS-472 - Handbook of Parameter Values for the Prediction of Radionuclide  
486 Transfer in Terrestrial and Freshwater Environments. International Atomic Energy  
487 Agency, Austria.

488 Krupka, K.M., Kaplan, D.I., Whelan, G., Serne, R.J., Mattigod, S.V. 1999. Understanding  
489 variation in partition coefficient,  $K_d$ , values. Volume 1: The  $K_d$  model, methods of  
490 measurement, and application of chemical reaction codes. Rep. No. EPA 402-R-99-004A.  
491 US Environmental Protection Agency, Washington, DC.

492 Nakao, A., Takeda, A., Ogasawara, S., Yanai, J., Ito, T. 2015. Relationship between paddy  
493 soil Radiocesium Interception Potentials and physicochemical properties in Fukushima,  
494 Japan. *J. Environ. Qual.* 44, 780-788.

495 Okumura, M., Kerisit, S., Bourg, I.C., Lammers, L.N., Ikeda, T., Sassi, M., Rosso, K.M.,  
496 Machida, M. 2018. Radiocesium interaction with clay minerals: Theory and simulation  
497 advances Post–Fukushima. *J. Environ. Radioact.* 189, 135-145.



498 Ohnuki, T., Kozai, N. 2013. Adsorption behavior of radioactive cesium by non-mica  
499 minerals. *J. Nucl. Sci. Technol.* 50, 369-375.

500 POSIVA, 2014. Working Report 2013-66 - Geochemical and physical properties, distribution  
501 coefficients of soils and sediments at the Olkiluoto Island and in the reference area in  
502 2010-2011. POSIVA, Finland.

503 Ramírez-Guinart, O., Kaplan, D., Rigol, A., Vidal, M. 2020a. Deriving probabilistic soil  
504 distribution coefficients ( $K_d$ ). Part 1: General approach to decreasing and describing  
505 variability and example using uranium  $K_d$  values. Submitted to *J. Environ. Radioactiv.*

506 Ramírez-Guinart, O., Kaplan, D., Rigol, A., Vidal, M. 2020b. Deriving probabilistic soil  
507 distribution coefficients ( $K_d$ ). Part 3: Reducing variability of americium  $K_d$  best estimates  
508 using soil properties and chemical and geological material analogues. Submitted to *J.*  
509 *Environ. Radioactiv.*

510 Rigol, A., Vidal, M., Rauret, G., 1998. Competition of organic and mineral phases in  
511 radiocesium partitioning in organic soils of Scotland and the area near Chernobyl.  
512 *Environ. Sci. Technol.* 32, 663-669.

513 Rigol, A., Vidal, M., Rauret, G., 2002. An overview of the effect of organic matter on soil-  
514 radiocaesium interaction: implications in root uptake. *J. Environ. Radioactiv.* 58, 191-216.

515 Roig, M., Vidal, M., Rauret, G., Rigol, A., 2007. Prediction of radionuclide aging in soils  
516 from the Chernobyl and Mediterranean areas. *J. Environ. Qual.* 36, 943-952.

517 Sheppard, S. C., 2011. Robust Prediction of  $K_d$  from Soil Properties for Environmental  
518 Assessment. *Hum. Ecol. Risk Assess.* 17(1), 263-279.

519 Simon-Cornu, M., Beaugelin-Seiller, K., Boyer, P., Calmon, P., Garcia-Sanchez, L.,  
520 Mourlon, C., Nicoulaud, V., Sy, M., Gonze, M.A. 2015. Evaluating Variability and  
521 Uncertainty in Radiological Impact Assessment Using SYMBIOSE. *J. Environ. Radioact.*  
522 139, 91-102.

523 SKB, 2014. TR-14-002 - Initial state report for the safety assessment SR-PSU. Svensk  
524 Kämbränslehantering AB-Swedish Nuclear Fuel and Waste Management Co, Sweden.

525 Söderlund, M., Virtanen, S., Välimaa, I., Lempinen, J., Hakanen, M., Lehto, J. 2016. Sorption  
526 of cesium on boreal forest soil II. The effect of time, incubation conditions, pH and  
527 competing cations. *J. Radioanal. Nucl. Chem.* 309, 647-657.

528 Sweeck, L., Wauters, J., Valcke, E., Cremers, A., 1990. In: Desmet, G., Nassibeni, P., Belli,  
529 M. (Eds.), *Transfer of radionuclides in natural and semi-natural environments*, New York,  
530 USA: Elsevier Applied Science Publishers.

531 Tarsitano, D., Young, S.D., Crout, N.M.J., 2011. Evaluating and reducing a model of  
532 radiocaesium soil–plant uptake. *J. Environ. Radioact.* 102, 262–269.

533 Uematsu, S., Smolders, E., Sweeck, L., Wannijn, J., Van Hees, M., Vandenhove, H., 2015.  
534 Predicting radiocaesium sorption characteristics with soil chemical properties for Japanese  
535 soils, *Sci. Total Environ.* 524-525, 148-156.

536 Vandebroek, L., van Hees, M., Delvaux, B., Spaargaren, O., Thiry, Y., 2012. Relevance of  
537 Radiocaesium Interception Potential (RIP) on a worldwide scale to assess soil vulnerability  
538 to <sup>137</sup>Cs contamination. *J. Environ. Radioactiv.* 102, 87-93.

539 Vidal, M., Roig, M., Rigol, A., Llauradó, M., Rauret, G., Wauters, J., Elsen, A., Cremers, A.,  
540 1995. Two approaches to the study of radiocaesium partitioning and mobility in  
541 agricultural soils from the Chernobyl area. *Analyst* 120, 1785-1791.

542 Waegeneers, N., Smolders, E., Merckx, R., 1999. A statistical approach for estimating the  
543 radiocaesium interception potential of soils. *J. Environ. Qual.* 28, 1005–1011.

544 Wampler, J. M., Krogstad E. J., Elliott W. C., Kahn B., Kaplan D.H., 2012. Long-term  
545 selective retention of natural Cs and Rb by highly weathered Coastal Plain soils. *Environ.*  
546 *Sci. Technol.* 46, 3837-3843.

547 Wang, G., Staunton, S. 2010. Dynamics of caesium in aerated and flooded soils:  
548 Experimental assessment of ongoing adsorption and fixation. *Eur. J. Soil Sci.* 61(6), 1005-  
549 1013.

550 Wauters, J., Elsen, A., Cremers, A., Konoplev, A. V., Bulgakov, A. A., Comans, R. N. J.,  
551 1996. Prediction of solid liquid distribution coefficients of radiocaesium in soils and  
552 sediments. Part 1: A simplified procedure for the solid characterisation, *Appl. Geochem.*  
553 11, 589–594.

554 **Table 1**555 Descriptors of Cs  $K_d$  ( $L\ kg^{-1}$ ) distributions after applying the initial OM+Texture criterion.

Partial dataset	N	GM	GSD	FLSD <sup>a</sup>	5 <sup>th</sup>	95 <sup>th</sup>
<i>Short-term</i>						
Overall	405	$2.2 \times 10^3$	5.7	A <sup>b</sup>	$5.2 \times 10^1$	$2.2 \times 10^4$
Organic	60	$1.8 \times 10^2$	6.1	B <sup>b</sup>	$2.0 \times 10^1$	$4.1 \times 10^3$
Mineral	345	$2.7 \times 10^3$	4.3	C <sup>b</sup>	$1.3 \times 10^2$	$2.4 \times 10^4$
Clay	32	$5.9 \times 10^3$	3.4	A <sup>c</sup>	$6.8 \times 10^2$	$3.5 \times 10^4$
Loam	190	$3.7 \times 10^3$	3.2	A <sup>c</sup>	$5.9 \times 10^2$	$2.6 \times 10^4$
Sand	110	$1.3 \times 10^3$	5.0	B <sup>c</sup>	$5.6 \times 10^1$	$1.0 \times 10^4$
<i>Long-term</i>						
Overall	168	$2.4 \times 10^4$	4.2	A <sup>d</sup>	$1.6 \times 10^3$	$1.5 \times 10^5$
Organic	20	$2.0 \times 10^3$	7.4	B <sup>d</sup>	$1.1 \times 10^2$	$9.2 \times 10^4$
Mineral	148	$2.8 \times 10^4$	2.6	C <sup>d</sup>	$6.8 \times 10^3$	$1.5 \times 10^5$

556 N = number of observations, GM = geometric mean, GSD = geometric standard deviation

557 <sup>a</sup> Different letters among the datasets compared indicate statistically significant differences between GMs558 according to the Fisher's Least Significant Differences test. Dataset comparisons shown here are: <sup>b</sup> short-term559 overall, mineral, and organic datasets; <sup>c</sup> short-term textural datasets; <sup>d</sup> long-term overall, mineral, and organic

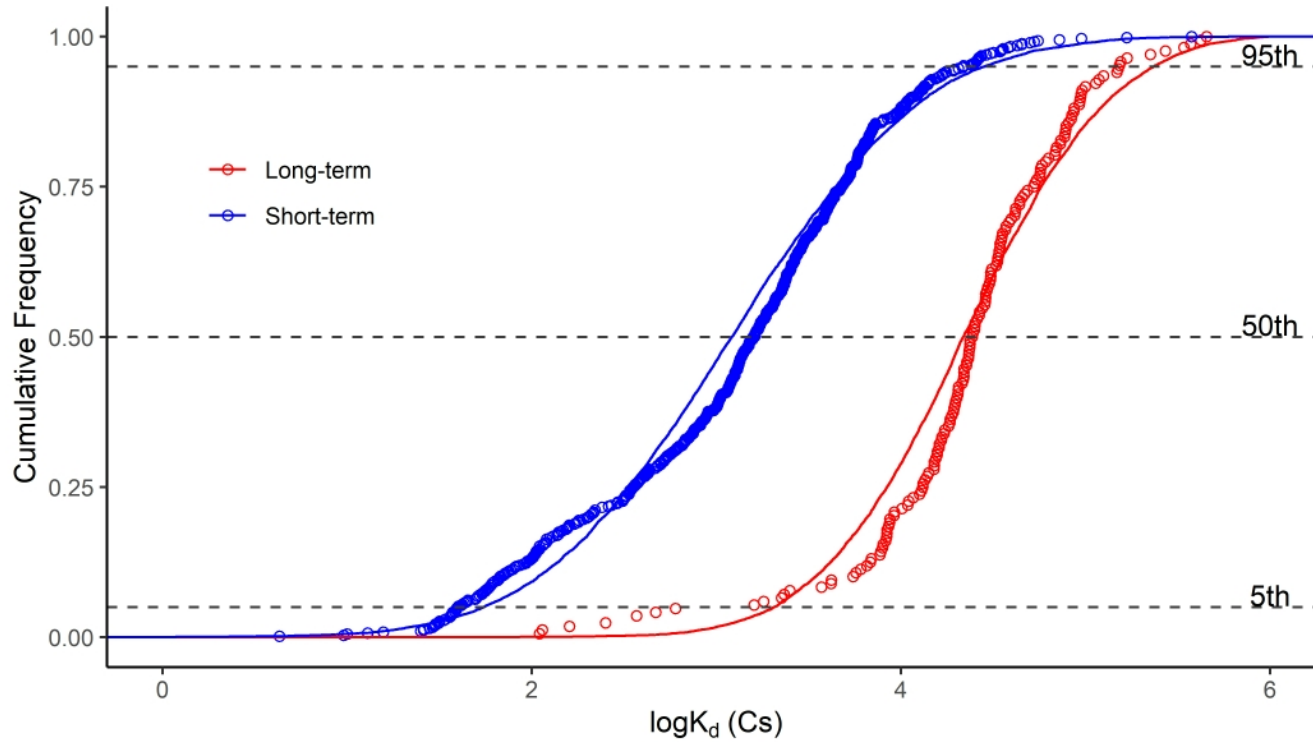
560 datasets.

561 **Figure captions**

562 **Fig. 1.** CDFs and descriptors of Cs  $K_d$  ( $L\ kg^{-1}$ ) distributions for soils grouped according to the  
563 Experimental Approach. Data for the Overall dataset are included for comparison. Points indicate  
564 individual dataset values whereas lines indicate the fitted distributions.

565 **Fig. 2.** CDFs and descriptors of Cs  $K_d$  ( $L\ kg^{-1}$ ) distributions for soils grouped according to RIP/ $K_{ss}$   
566 criterion. Points indicate individual dataset values whereas lines indicate the fitted distributions.

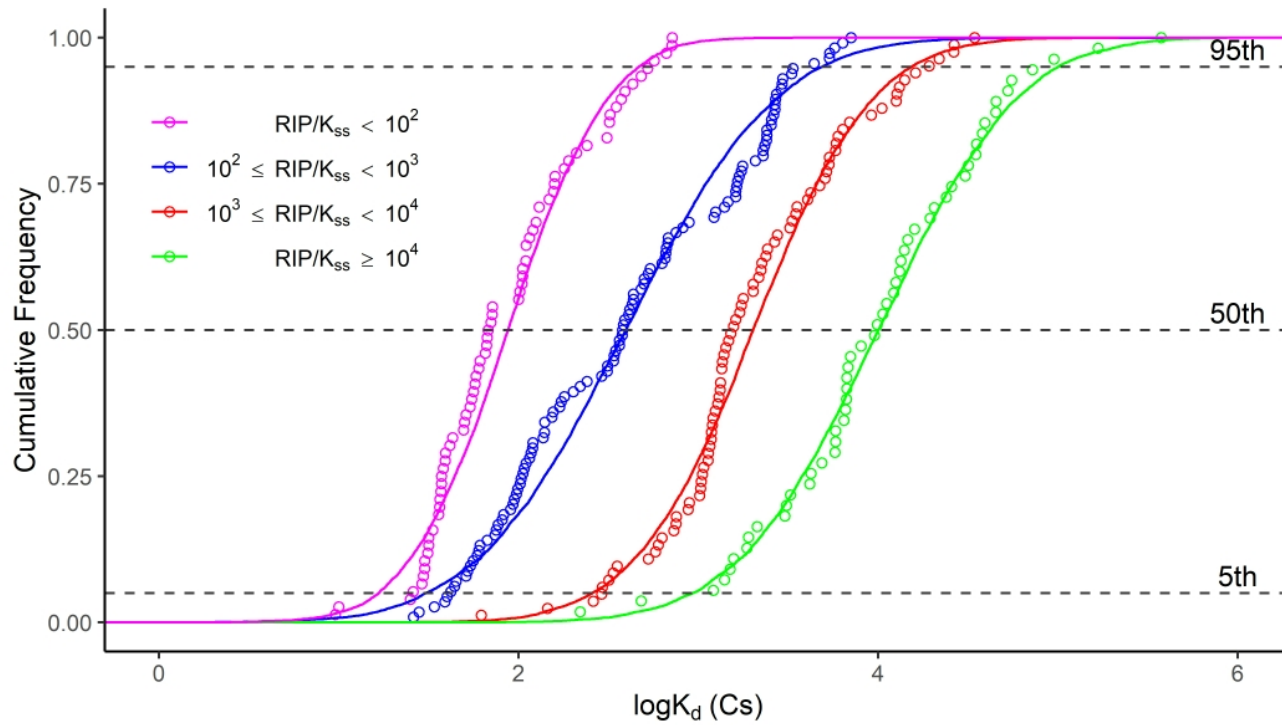
567 **Fig. 3.** CDFs and descriptors of Cs  $K_d$  ( $L\ kg^{-1}$ ) distributions derived from the redefined OM+Texture  
568 criterion for short-term (A) and long-term (B) partial datasets. Points indicate individual dataset values  
569 whereas lines indicate the fitted distributions.



Partial dataset	N	GM	GSD	FSLD <sup>a</sup>	5 <sup>th</sup>	95 <sup>th</sup>
Overall	769	$2.5 \times 10^3$	8.6		$5.0 \times 10^1$	$6.3 \times 10^4$
Short-term	601	$1.6 \times 10^3$	6.6	A	$4.0 \times 10^1$	$2.2 \times 10^4$
Long-term	168	$2.4 \times 10^4$	4.2	B	$1.6 \times 10^3$	$1.5 \times 10^5$

N = number of observations, GM = geometric mean, GSD = geometric standard deviation

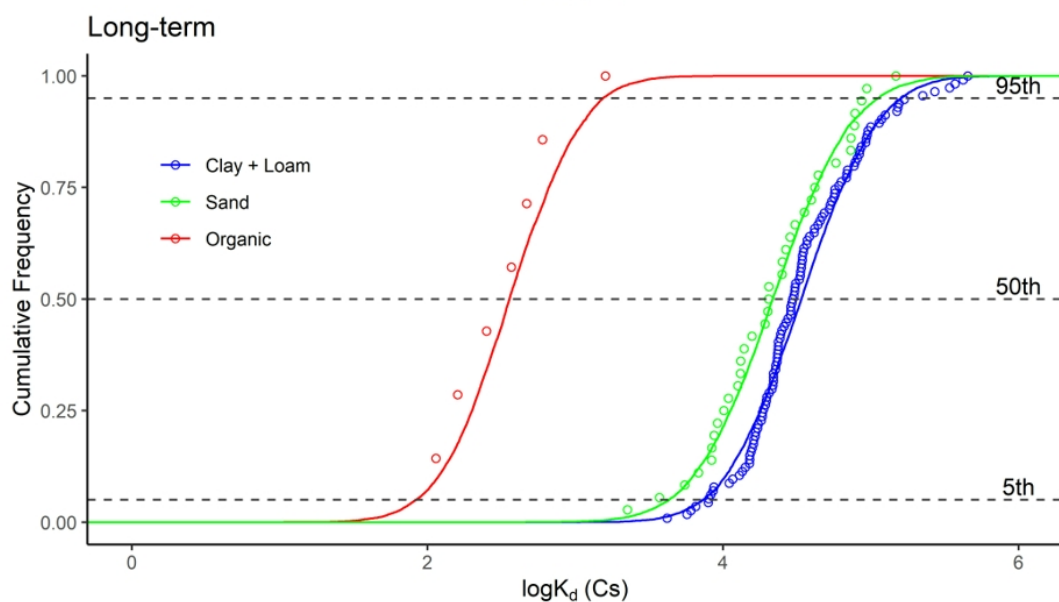
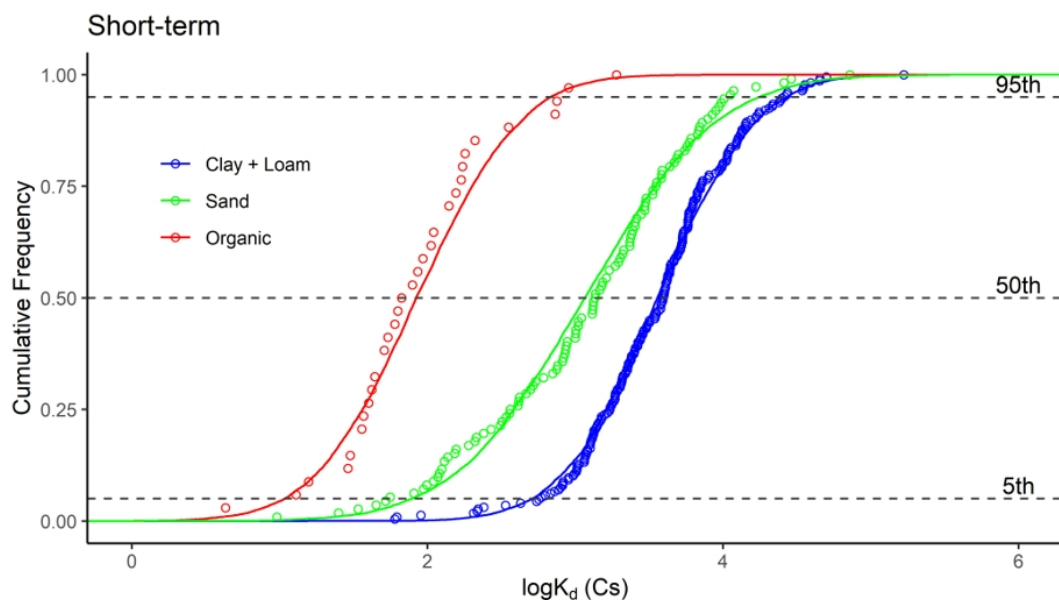
<sup>a</sup> Different letters among the datasets compared indicate statistically significant differences between GMs according to the Fisher's Least Significant Differences test.



Partial dataset	N	GM	GSD	FLSD <sup>a</sup>	5 <sup>th</sup>	95 <sup>th</sup>
RIP/K <sub>ss</sub> < 10 <sup>2</sup>	74	6.9 × 10 <sup>1</sup>	2.7	A	2.6 × 10 <sup>1</sup>	5.7 × 10 <sup>2</sup>
10 <sup>2</sup> ≤ RIP/K <sub>ss</sub> < 10 <sup>3</sup>	116	3.8 × 10 <sup>2</sup>	4.5	B	4.2 × 10 <sup>1</sup>	4.4 × 10 <sup>3</sup>
10 <sup>3</sup> ≤ RIP/K <sub>ss</sub> < 10 <sup>4</sup>	83	1.6 × 10 <sup>3</sup>	3.4	C	2.9 × 10 <sup>2</sup>	1.9 × 10 <sup>4</sup>
RIP/K <sub>ss</sub> ≥ 10 <sup>4</sup>	55	1.0 × 10 <sup>4</sup>	4.1	D	1.2 × 10 <sup>3</sup>	9.5 × 10 <sup>4</sup>

N = number of observations, GM = geometric mean, GSD = geometric standard deviation

<sup>a</sup> Different letters among the datasets compared indicate statistically significant differences between GMs according to the Fisher's Least Significant Differences test.



Partial dataset	N	GM	GSD	FLSD <sup>a</sup>	5 <sup>th</sup>	95 <sup>th</sup>
<i>Short-term</i>						
Mineral (OM < 50%)	367	$2.5 \times 10^3$	4.5	A <sup>b</sup>	$1.2 \times 10^2$	$2.4 \times 10^4$
Clay+Loam	227	$3.9 \times 10^3$	3.3	B <sup>b</sup>	$5.9 \times 10^2$	$2.6 \times 10^4$
Sand	112	$1.4 \times 10^3$	5.2	C <sup>b</sup>	$5.6 \times 10^1$	$1.1 \times 10^4$
Organic (OM ≥ 50%)	38	$8.9 \times 10^1$	4.2	D <sup>b</sup>	$1.3 \times 10^1$	$1.9 \times 10^3$
<i>Long-term</i>						
Mineral (OM < 90%)	161	$2.5 \times 10^4$	3.2	A <sup>c</sup>	$4.2 \times 10^3$	$1.5 \times 10^5$
Clay+Loam	114	$3.0 \times 10^4$	2.6	B <sup>c</sup>	$8.0 \times 10^3$	$2.2 \times 10^5$
Sand	36	$2.0 \times 10^4$	2.7	A <sup>c</sup>	$3.7 \times 10^3$	$9.4 \times 10^4$
Organic (OM ≥ 90%)	7	$3.7 \times 10^2$	2.4	C <sup>c</sup>	$1.1 \times 10^2$	$1.6 \times 10^3$

N = number of observations, GM = geometric mean, GSD = geometric standard deviation

<sup>a</sup> Different letters among the datasets compared indicate statistically significant differences between GMs according to the Fisher's Least Significant Differences test. Dataset comparisons shown here are:

<sup>b</sup> short-term mineral, textural and organic datasets; <sup>c</sup> long-term mineral, textural and organic datasets.

## **SUPPLEMENTARY MATERIAL**

**Deriving probabilistic soil distribution coefficients ( $K_d$ ). Part 2: Reducing caesium  $K_d$  uncertainty by accounting for experimental approach and soil properties**



**Table S1**

Examination of the effect of the OM threshold in deriving Mineral and Organic datasets.

OM Threshold (%)	Mineral				Organic			
	N	GM	GSD	FLSD <sup>a</sup>	N	GM	GSD	FSLD <sup>a</sup>
<i>Short term</i>								
20	345	$2.7 \times 10^3$	4.3	A <sup>b</sup>	60	$1.8 \times 10^2$	6.1	A <sup>d</sup>
30	355	$2.4 \times 10^3$	4.3	A <sup>b</sup>	50	$1.5 \times 10^2$	5.8	AB <sup>d</sup>
40	360	$2.3 \times 10^3$	4.5	A <sup>b</sup>	45	$1.2 \times 10^2$	4.6	AB <sup>d</sup>
50	367	$2.3 \times 10^3$	4.5	A <sup>b</sup>	38	$8.9 \times 10^1$	4.2	B <sup>d</sup>
<i>Long term</i>								
20	148	$2.8 \times 10^4$	2.6	A <sup>c</sup>	20	$2.0 \times 10^3$	7.4	A <sup>e</sup>
60	150	$3.1 \times 10^4$	2.6	A <sup>c</sup>	18	$1.2 \times 10^3$	4.9	AB <sup>e</sup>
70	153	$2.9 \times 10^4$	3.0	A <sup>c</sup>	15	$1.2 \times 10^3$	4.6	AB <sup>e</sup>
80	154	$2.9 \times 10^4$	3.0	A <sup>c</sup>	14	$1.1 \times 10^3$	4.5	AB <sup>e</sup>
90	161	$2.5 \times 10^4$	3.2	A <sup>c</sup>	7	$3.7 \times 10^2$	2.4	B <sup>e</sup>

N = number of observations, GM = geometric mean, GSD = geometric standard deviation

<sup>a</sup> Different letter among the datasets compared indicate statistically significant differences according to the Fisher's Least Significant Differences test. Dataset comparisons shown here are: <sup>b</sup> short-term mineral datasets; <sup>c</sup> long-term mineral datasets; <sup>d</sup> short-term organic datasets; <sup>e</sup> long-term organic datasets.

**Figure S1**

Plots of  $\log K_d$  vs.  $\log (RIP/K_{ss})$  and  $\log K_d$  vs.  $\log K_{d,pred}$  ( $K_{d,pred}$ : calculated from equation [3]).

